

Title	Tunable L-band semiconductor laser based on Mach-Zehnder interferometer
Authors	Dernaika, Mohamad;Caro, Ludovic;Kelly, Niall P.;Shayesteh, Maryam;Peters, Frank H.
Publication date	2017-07-04
Original Citation	Dernaika, M., Caro, L., Kelly, Niall P., Shayesteh, M. and Peters, Frank H. (2017) 'Tunable L-band semiconductor laser based on Mach-Zehnder interferometer', Optics Communications, 402, pp. 56-59. doi: 10.1016/j.optcom.2017.05.073
Type of publication	Article (peer-reviewed)
Link to publisher's version	10.1016/j.optcom.2017.05.073
Rights	© 2017 The Authors. Published by Elsevier B.V. This is an open access article under the CC BY-NC-ND license ( <a href="http://creativecommons.org/licenses/by-nc-nd/4.0/">http://creativecommons.org/licenses/by-nc-nd/4.0/</a> ). - <a href="http://creativecommons.org/licenses/by-nc-nd/4.0/">http://creativecommons.org/licenses/by-nc-nd/4.0/</a>
Download date	2024-04-25 14:27:45
Item downloaded from	<a href="https://hdl.handle.net/10468/4276">https://hdl.handle.net/10468/4276</a>



# UCC

**University College Cork, Ireland**  
 Coláiste na hOllscoile Corcaigh



# Tunable L-band semiconductor laser based on Mach–Zehnder interferometer

Mohamad Dernaika<sup>a,b,\*</sup>, Ludovic Caro<sup>a,c</sup>, Niall P. Kelly<sup>a,c</sup>, Maryam Shayesteh<sup>a</sup>, Frank H. Peters<sup>a,c</sup>

<sup>a</sup> Integrated Photonics Group, Tyndall National Institute, Dyke Parade, Cork, Ireland

<sup>b</sup> Electrical and Electronic Engineering Department, University College Cork, College Road, Cork, Ireland

<sup>c</sup> Physics Department, University College Cork, College Road, Cork, Ireland

## ARTICLE INFO

MSC:  
00-01  
99-00

### Keywords:

Semiconductor laser  
Photolithography  
L-band  
Single mode  
Lasers  
Mach–Zehnder interferometer

## ABSTRACT

A regrowth-free tunable L-band semiconductor laser based on Mach–Zehnder interferometer is presented in this paper. The laser exhibit a side mode suppression ratio of 38 dB and linewidth of 500 kHz. A tuning range of 30 nm across the L-band is also demonstrated.

© 2017 The Authors. Published by Elsevier B.V. This is an open access article under the CC BY-NC-ND license (<http://creativecommons.org/licenses/by-nc-nd/4.0/>).

## 1. Introduction

The dramatic growth of Internet traffic and services requiring high data rates have created a demand for ever increasing bandwidth. The current dense wavelength division multiplexing (DWDM) networks need to expand beyond the C-band in order to improve the network capacity. Hence, the L-band optical window has been a subject of great interest due to its potential to increase the network bandwidth and flexibility [1–5].

Distributed feedback (DFB) and distributed Bragg reflector (DBR) lasers deliver a stable single mode operation in the L-band [6–8]. However, they require epitaxial re-growth, high resolution lithography such as electron beam (E-beam) and complex cavity designs to reduce the laser linewidth [9,10].

Regrowth-free semiconductor lasers fabrication process that employ standard UV lithography have attracted a lot of interest due to their potential to significantly reduce fabrication cost, time and complexity. Various designs and approaches were reported such as coupled cavities [11], rings [12], and slots [13] to create a tunable single mode laser mostly covering the C-band. Other than in addition to greatly reducing the overall fabrication cost and time, these lasers provide a tunable output, high side mode suppression ratio (SMSR) and sub-MHz narrow linewidth suitable for advanced modulation formats.

In this paper we demonstrated a L-band semiconductor laser based on an active Mach–Zehnder interferometer (MZI). The laser is fabricated using a regrowth-free process and standard UV lithography. The MZI achieves a SMSR of 38 dB and linewidth of 500 kHz without the need of complicated cavity designs, external cavity or high reflection (HR) coating. A tuning range over 30 nm across the L-band is demonstrated.

## 2. Design and fabrication

The MZI laser cavity consist of two  $1 \times 2$  multimode interference (MMI) couplers used to split/combine two asymmetric pathways resonating between the two cleaved facets. The MZI operation is achieved by exploiting the relative path length differences of the light traveling in the two asymmetric pathways. The constructive and destructive wavelength dependent interference creates a response similar to a filter allowing only the constructively interfered modes to lase. Moreover, only the mode that coincide with the gain peak of the laser material will dominate the transmission leading to a single mode operation.

A microscope image of the device is shown in Fig. 1(a) showing the 4-section laser with the separate metal pads. Fig. 1(b) shows an illustration of the design, which includes: the deeply etched area inside the green squares, the isolation slots and the MMIs used to split and

\* Corresponding author at: Integrated Photonics Group, Tyndall National Institute, Dyke Parade, Cork, Ireland.  
E-mail address: [Mohamad.Dernaika@Tyndall.ie](mailto:Mohamad.Dernaika@Tyndall.ie) (M. Dernaika).

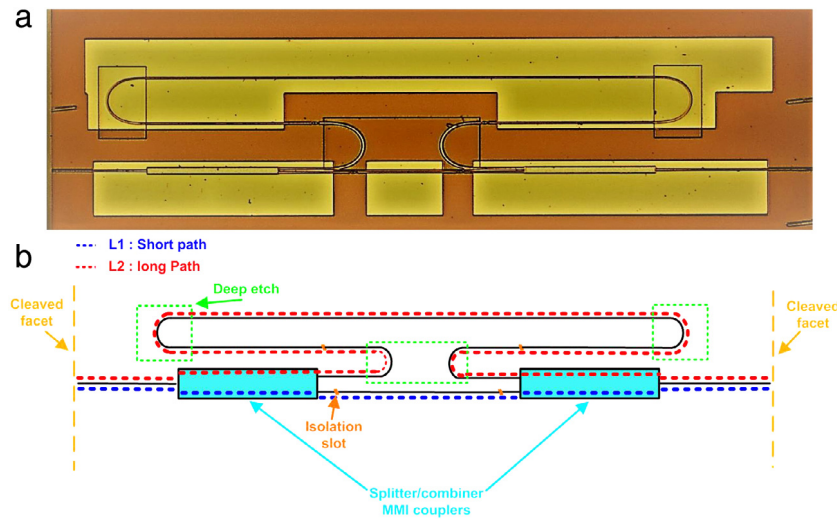


Fig. 1. (a) Microscope image of the MZI laser consisting of 2 MMI's and asymmetric arms (b) design illustration of the MZI laser cavity. (For interpretation of the references to color in this figure legend, the reader is referred to the web version of this article.)

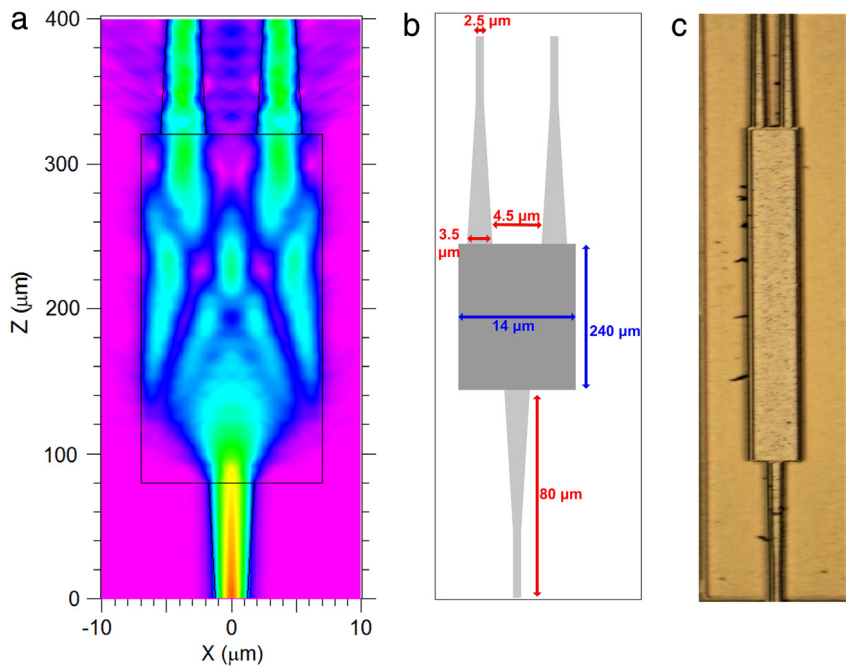


Fig. 2. (a) Simulation of the 1 × 2 MMI coupler (b) MMI dimensions (c) 1 × 2 MMI microscope image.

combine the light. The short and long paths of the MZI (L1 and L2) are illustrated as the blue and red dotted lines respectively with a  $\Delta L$  of  $\approx 2$  mm. The interference occurs when both cavities with the relative phase different are combined at the MMIs. Moreover, the deeply etched, high curvature bends were used to significantly reduce the footprint of the device which is  $400 \times 1300 \mu\text{m}$ . The green squares in Fig. 1(b) represent the deeply etched regions used to minimize the bending loss by increasing the refractive index contrast, and thus ensuring stronger mode confinement. The laser was divided into 4 sections, each with a separate metal pad. The different sections were separated using an isolation slot with a 7-degree angle to reduce unwanted reflections. The MMI couplers are critical components in the MZI cavity, as high loss couplers will significantly affect the laser performance in term of output power, SMSR and linewidth. Therefore, the MMI coupler was simulated using a 3D model of the epitaxial material used to fabricate the laser to ensure optimal performance. The MMI dimensions and input/output waveguides were calculated and optimized using the

commercial software BeamProp from Rsoft, which employs the well-established beam propagation method.  $80 \mu\text{m}$  long tapered waveguides were used at the input and the output of the coupler to optimize the power coupling. The waveguides were tapered from  $2.5$  to  $3.5 \mu\text{m}$ . The length and the width of the MMI couplers was  $240$  and  $14 \mu\text{m}$  respectively. Fig. 2(a) shows the simulation model of the  $1 \times 2$  MMI and the relevant dimensions are presented in Fig. 2(b) along a microscope image of the coupler Fig. 2(c).

A theoretical model using scattering matrix method (SMM) [14] was developed to simulate the cavity design shown in Fig. 3(a). The model take in consideration the resonance between the 2 cleaved facets and the phase difference between the MZI arms. A detailed description of the SMM technique used can be found in [15]. The simulated optical spectrum in Fig. 3(b) shows the transmission as a function of the wavelength across  $20 \text{ nm}$  generated using the SMM technique. The MZI cavity results in a free spectral range of  $\sim 1.5 \text{ nm}$ , which is sufficient for strong single mode operation when the gain is centered at a resonance.

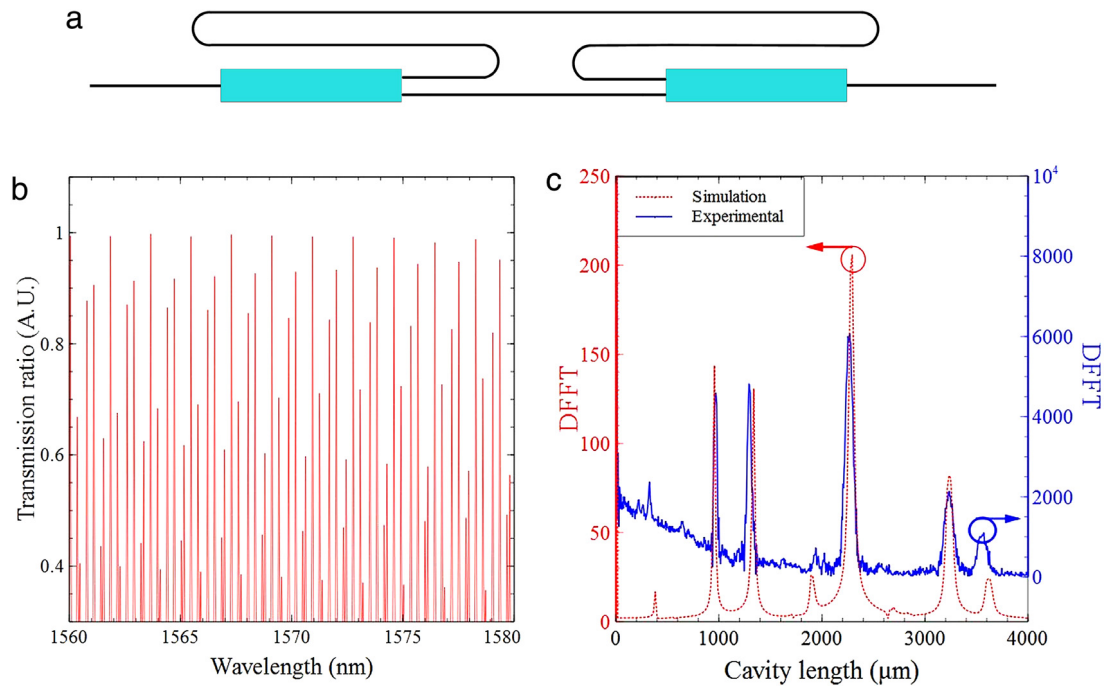


Fig. 3. (a) MZI path ways illustration (b) simulated optical transmission spectrum of the MZI cavity (c) FFT cavity analysis.

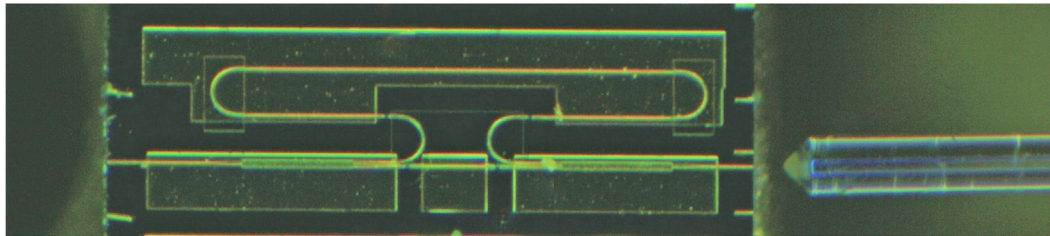


Fig. 4. Microscope image of the DUT.

The blue line in Fig. 3(c) shows the experimental fast Fourier transform (FFT) cavity analysis extracted from the near threshold optical spectrum of the laser. The peaks represent the short and long path length of the laser and the corresponding coupled cavities resulting from the interaction of the 2 cleaved facets and the MZI arms. Furthermore, the red dotted line in Fig. 3(b) shows the FFT cavity analysis of the theoretical optical resonance model, which shows excellent agreement with the experimental data. This suggests that the developed theoretical model can be used to predict the behavior of such cavities for further optimization and analysis purposes.

The laser material used was commercially available IQE epitaxy that consist of a multiple quantum well (QW) structure on a n-doped substrate. The epitaxial structure have an active region with a total thickness of 400 nm that comprise  $5 \times 6$  nm AlInGaAs strained QWs and  $6 \times 10$  nm barriers. The upper cladding layer consist of a 20 nm GaInAsP etch stop layer, a 1580 nm InP and finally a 50 nm GaInAsP and 200 nm GaInAs metal contact layers. Two depth levels were used in the process, shallow and deep. The 1.8  $\mu\text{m}$  shallow etch depth was used to define the ridge and the isolation slots. Whereas, the 3  $\mu\text{m}$  deep etch, that goes through the active region down to the n-doped substrate, is used to define the bends. The dry etch process employed the following recipe to ensure a smooth side walls:  $\text{CL}_2/\text{CH}_4/\text{H}_2$ . The deposited backside N metal is 20:250 Ti: Au and the P metal used is 20:350 nm Ti: Au deposited using  $360^\circ$  rotation to ensure that side walls are fully covered with gold. Finally, the substrate was thinned to 110  $\mu\text{m}$  using bromine methanol solution and annealed at  $380^\circ$  for 5 min to improve the metal adhesion and reduce the device resistivity.

### 3. Results

Four individual probes were used to inject current into the device under test (DUT). The light was coupled into a lensed fiber from one of the two cleaved facets as shown in Fig. 4. An output power  $>1$  mW was measured at various wavelengths. The DUT was placed on a temperature controlled brass chuck with a fixed temperature of  $20^\circ\text{C}$ . The collected light was then connected to an inline power meter and then to a optical spectrum analyzer (OSA) via the lensed fiber. The single mode operation of the MZI laser can be seen in Fig. 5.

The laser achieves an SMSR of 38 dB as shown in Fig. 5(a). Moreover, the laser is tunable from 1584 nm 1615 nm covering 30 nm across the L-band. The tuning was achieved by increasing the injected current into the MZI, and an SMSR between 33 and 38 dB was maintained across the tuning range. The tuning is achieved by increasing the injection current which cause a slight change in the refractive index of the material. A further increase in the current give rise to thermal effects which cause a red shift to the resonating cavity modes allowing a wide tuning range.

The MZI laser linewidth was measured using a delayed self-heterodyne setup employing 50 km fiber delay line in a recirculating loop configuration [16].

The experimental setup used to measure the linewidth is shown in Fig. 6(a). A 90/10 coupler was used to split the light output. The 90% portion of the light propagate through the re-circulating loop mirror. The loop comprises of a 50 km single mode fiber delay line, followed by a  $>30$  dB isolator. Next an 80 MHz acousto-optic modulator is used to frequency shift the signal before going into a Polarization controller.

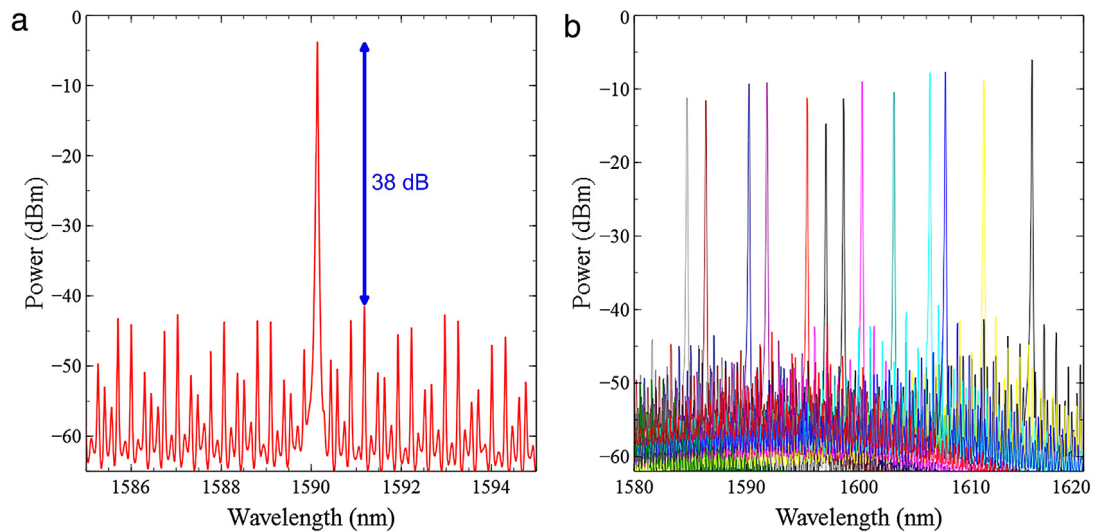


Fig. 5. (a) SMSR of 38 dB (b) tuning over 30 nm.

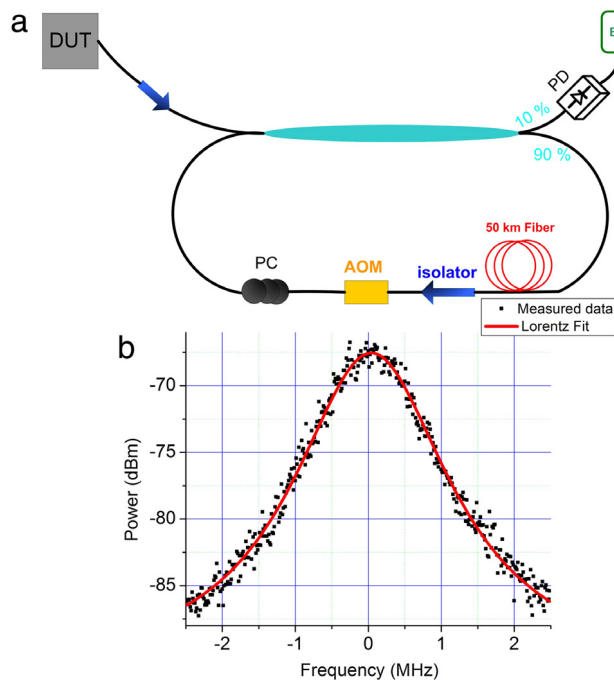


Fig. 6. (a) Re-circulating loop linewidth measurement setup (b) 500 kHz linewidth of the MZI laser.

The shifted signal from the loop is recombined with the original signal and is measured by a 10 MHz–1 GHz photodiode (PD) with a wavelength range of 850–1650 nm. Finally, a 22 GHz electrical spectrum analyzer (ESA) was used to detect the beat signal. Fig. 6(b) shows the 1 MHz beat signal which corresponds to a 500 kHz Laser linewidth.

#### 4. Conclusion

This paper demonstrated a tunable L-band semiconductor laser based on a MZI suitable for optical communication. The laser achieves a SMSR

of 38 dB and linewidth of 500 kHz. Moreover the MZI covers 30 nm tuning range over the L-band extending from 1585 to 1615 nm.

#### References

- [1] H. Choi, J. Oh, D. Lee, S. Ahn, B. Park, S. Lee, Simple and efficient L-band erbium-doped fiber amplifiers for WDM networks, *Opt. Commun.* 213 (2002) 63–66.
- [2] C.-L. Zhao, S. Yang, H. Meng, Z. Li, S. Yuan, K. Guiyun, X. Dong, Efficient multi-wavelength fiber laser operating in L-band, *Opt. Commun.* 204 (2002) 323–326.
- [3] H. Sakata, H. Yoshimi, Y. Otake, Wavelength tunability of L-band fiber ring lasers using mechanically induced long-period fiber gratings, *Opt. Commun.* 282 (2009) 1179–1182.
- [4] B.-H. Choi, I.-B. Kwon, A wide tunable fiber laser for two independent C-band and L-band wavelengths, *Opt. Commun.* 286 (2013) 156–160.
- [5] G.-R. Lin, J.-Y. Chang, Y.-S. Liao, H.-H. Lu, L-band erbium-doped fiber laser with coupling-ratio controlled wavelength tunability, *Opt. Express* 14 (2006) 9743–9749.
- [6] M. Funabashi, High power DFB lasers covering L-band, in: *Lasers and Electro-Optics Society, 2003, LEOS 2003, The 16th Annual Meeting of the IEEE*, vol. 1, IEEE, 2003, pp. 196–197.
- [7] H. Ishii, H. Oohashi, K. Kasaya, K. Tsuzuki, Y. Tohmori, High-power (40 mW) L-band tunable DFB laser array module using current tuning, in: *Optical Fiber Communication Conference, Optical Society of America, 2005*, p. OTuE1.
- [8] S.H. Oh, K.-H. Yoon, K.S. Kim, J. Kim, O.-K. Kwon, D.K. Oh, Y.-O. Noh, H.-J. Lee, L-band tunable external cavity laser based on 1.58  $\mu\text{m}$  superluminescent diode integrated with spot-size converter, *Opt. Express* 18 (2010) A300–A306.
- [9] T. Komljenovic, S. Srinivasan, E. Norberg, M. Davenport, G. Fish, J.E. Bowers, Widely tunable narrow-linewidth monolithically integrated external-cavity semiconductor lasers, *IEEE J. Select. Topics Quant. Electron.* 21 (2015) 214–222.
- [10] W. Lewoczko-Adamczyk, C. Pyrlík, J. Häger, S. Schwertfeger, A. Wicht, A. Peters, G. Erbert, G. Tränkle, Ultra-narrow linewidth DFB-laser with optical feedback from a monolithic confocal Fabry-Perot cavity, *Opt. Express* 23 (2015) 9705–9709.
- [11] P.E. Morrissey, N. Kelly, M. Dernaika, L. Caro, H. Yang, F.H. Peters, Coupled cavity single-mode laser based on regrowth-free integrated MMI reflectors, *IEEE Photon. Technol. Lett.* 128 (2016) 1313–1316.
- [12] S.-H. Kim, Y.-T. Byun, D.-G. Kim, N. Dagli, Y.-C. Chung, Widely tunable coupled-ring reflector laser diode consisting of square ring resonators, *J. Opt. Soc. Korea* 14 (2010) 38–41.
- [13] K. Shi, F. Smyth, D. Reid, B. Roycroft, B. Corbett, F. Peters, L. Barry, Characterization of a tunable three-section slotted Fabry-Perot laser for advanced modulation format optical transmission, *Opt. Commun.* 284 (2011) 1616–1621.
- [14] L. Coldren, S. Corzine, M. Maanovi, *Diode Lasers and Photonic Integrated Circuits*, John Wiley and Sons, Inc., 2012.
- [15] L. Caro, N.P. Kelly, M. Dernaika, M. Shayesteh, P.E. Morrissey, J.K. Alexander, F.H. Peters, A facetless regrowth-free single mode laser based on MMI couplers, *Opt. Laser Technol.* 94 (2017) 159–164.
- [16] H. Tsuchida, Simple technique for improving the resolution of the delayed self-heterodyne method, *Opt. Lett.* 15 (1990) 640–642.